Hindawi Publishing Corporation
Journal of Nanomaterials
Volume 2012, Article ID 674104, 7 pages
doi:10.1155/2012/674104

Research Article

Fabrication and Characterization of Composite Containing HCl-Doped Polyaniline and Fe Nanoparticles

Rongcheng Liu,[1] Hong Qiu,[1] Hua Zong,[1] and Chunying Fang[2]

[1] *Department of Physics, School of Mathematics and Physics, University of Science and Technology Beijing, 30 Xueyuan Road, Haidian District, Beijing 100083, China*
[2] *Department of Chemistry, School of Chemistry and Biological Engineering, University of Science and Technology Beijing, 30 Xueyuan Road, Haidian District, Beijing 100083, China*

Correspondence should be addressed to Hong Qiu, qiuhong@sas.ustb.edu.cn

Received 24 October 2011; Accepted 12 December 2011

Academic Editor: Makis Angelakeris

HCl-doped polyaniline powder (HCl-PANI) was synthesized by using a polymerization procedure. Fe nanoparticles were then deposited on the HCl-PANI at room temperature by direct current magnetron sputtering. After this process the HCl-PANI-Fe composite was obtained. Fe nanoparticle size in the composite is about 100 nm. HCl-PANI structure is not influenced by the Fe nanoparticles. The composite pellet has room temperature ferromagnetism and a conductivity of 0.25 S/cm. Temperature dependence of the conductivity reveals that a carrier transport mechanism in the composite is three-dimensional variable range hopping. Thermogravimetric analysis reveals that a weight loss of the HCl-PANI-Fe composite is smaller than that of the HCl-PANI for the same heating temperature when the temperature exceeds 230°C.

1. Introduction

Polyaniline (PANI) having both electrical and magnetic features has attracted considerable attention for its potential applications in electrical, magnetic, and electronic devices as well as stealth technology and electromagnetic interference shielding. The conductive and magnetic PANI composites containing iron oxides such as Fe_3O_4 and Fe_2O_3 were mostly studied, for example, see references [1–10]. As it is well known, pure Fe is easily oxidized in moist or oxidizing atmosphere. Thus it is a challenging work to prepare the conductive PANI composites containing Fe (PANI-Fe). Izumi et al. [11] chemically polymerized PANI doped with Fe and found the formation of semiquinone segments upon coordination of emeraldine base PANI to Fe^{3+} ions. Li et al. [12] prepared the PANI-Fe polymer at room temperature by chemical synthesis in the absence and presence of an applied magnetic field. The PANI-Fe polymer was a complex rather than a composite in which Fe nanoparticles were covered by PANI. The PANI-Fe complex polymer had both conductive and ferromagnetic behaviors. Fe^{3+} ions coordinated mainly with the nitrogen atoms on the quinone rings. Xue et al. [13] mechanically mixed PANI doped with 4-dodecylbenzenesulfonic acid (DBSA) and Fe nanoparticles obtaining DBSA-PANI-Fe composites. As the Fe nanoparticle content increased from 0 to 70 wt%, a conductivity of the composite pellet decreased linearly from 0.25 to 0.07 S/cm and the saturation magnetization increased monotonically to 78 emu/g. However, the Fe nanoparticles were partly oxidized forming iron oxides which were detected by X-ray diffraction [13]. Thus, in the strict sense, Xue et al. prepared the DBSA-PANI-Fe-Fe_3O_4 composites.

Sputter deposition is one of the most important techniques for preparing the thin film because the purity of the film can be easily controlled and the adhesion of the film to the substrate can be enhanced. The magnetron sputtering technique can trap electrons in the region near the target and can effectively ionize working gas, leading to fast deposition of the film at room temperature. It was reported that sputter deposition could prepare dense and pure Fe thin films and islands [14, 15]. On the basis of the above-mentioned advantage of sputter deposition, it is desirable to prepare PANI-Fe composites by sputter-depositing Fe islands or particles on the PANI. Recently, HCl-PANI-Ni composites

have been successfully prepared using the well-established polymerization procedure followed by sputter-deposition of Ni, that is, using the chemically and physically combinative method [16]. The HCl-PANI-Ni composites had the conductive and ferromagnetic features. In the present work, HCl-doped polyaniline powder (HCl-PANI) is synthesized by using a polymerization procedure. Fe nanoparticles are deposited on the HCl-PANI at room temperature by direct current (DC) magnetron sputtering. After this process, the HCl-PANI-Fe composite is obtained. Structural, magnetic, and electrical properties of the composite are studied. This work, besides fabrication and study of the HCl-PANI-Fe composite, will further confirm the feasibility of the chemically and physically combinative method to prepare the PANI composites containing metal nanoparticles.

2. Experimental Procedure

2.1. Preparation of HCl-PANI-Fe Composite. All the reagents were purchased from Beijing Chemical Works and were analytical grade. Only aniline was doubly distilled under reduced pressure and stored in refrigerator (at about 4°C) prior to using. The other reagents were used without further purification. HCl-PANI was chemically synthesized using the well-established polymerization procedure [17]. Aniline (0.1 mol) was dissolved in 100 mL aqueous hydrochloric acid (HCl, 1 mol/L) taken in a three-neck flask. The mixture solution was cooled and stirred at −3°C by a magnetic stirrer. Then 51.5 mL ammonium persulfate solution (2.4 mol/L) in a constant pressure funnel was slowly added into the mixture solution for 1 hour in order to avoid heating the reaction mixture. The reaction proceeded at −3°C for 8 hours. The final solution was filtered. The precipitate was washed with aqueous HCl (1 mol/L) for protonating. The protonated precipitate was washed with deionized water and acetone until the washing water and acetone became colorless. Then the powder was dried at 50°C in vacuum for two days. The HCl-PANI powder was obtained.

The HCl-PANI powder was compacted to pellets with 0.2 mm in thickness and 50 mm in diameter. Fe particles or thin films were deposited on the two surfaces of the HCl-PANI pellet at room temperature by using a DC magnetron sputtering system (KYKY Technology Development). The Fe target (99.99% in purity) with 50 mm in diameter was inclined at an angle of 45° to the pellet. The distance between the target and the pellet was about 100 mm. The pellet holder was rotated using a stepping motor during deposition in order to obtain the uniform distribution of Fe particles or the uniform thickness of Fe thin film. Prior to deposition, the working chamber was evacuated to a pressure lower than 2×10^{-4} Pa using a turbo molecular pump. An Ar gas (99.9995% in purity) pressure was 1.0 Pa and a sputtering power applied to the target was fixed at 100 W. The deposition rate was about 12 nm/min and the deposition time was 10 minutes.

In order to obtain the HCl-PANI-Fe composite, the HCl-PANI pellet sputter-deposited Fe particles or thin film was mechanically milled at an almost same speed in an agate mortar for 30 minutes in ambient air. According to the Fe deposition amount and the pellet mass, the nominal Fe content in the HCl-PANI-Fe composite was estimated to be about 1.66 wt%. The composite powder was compacted to pellets with 0.5 mm in thickness and 13 mm in diameter at a same pressure.

2.2. Analysis of HCl-PANI-Fe Composite. X-ray diffraction (XRD) (Rigaku, D/Max-RB) was used to analyze the structure of the HCl-PANI-Fe composite. The XRD measurements were performed in a standard θ–2θ scan using a Cu Kα radiation filtered by a crystal monochromator (wavelength $\lambda = 0.15406$ nm). Transmission electron microscopy (TEM) (Philips, F20) was used to observe the structure of the Fe particles in the composite. The molecular structure of the composite was characterized by Fourier transform infrared spectroscope (FT-IR) (Nexus, 670). A magnetization curve of the composite pellet was measured at room temperature using a vibrating sample magnetometer (VSM) (Quantum Design, Versalab). The magnetic field was applied along the pellet plane during the VSM measurement. A temperature dependence of the magnetization for the HCl-PANI-Fe composite pellet was measured from 55 K to 300 K. First, the composite pellet was cooled down to 55 K at zero field. Then the magnetization data were taken with warming up under a magnetic field of 1000 Oe applied along the pellet plane. The warming rate was approximate to 4 K/min. The magnetization data of the HCl-PANI-Fe composite was estimated by subtracting the signal of the sample holder. Resistance R of the HCl-PANI-Fe composite pellet was measured at room temperature using a four-point probe technique. The spacing between the two adjacent probe tips was 3 mm. The conductivity σ of the composite pellet can be given by [18]

$$\sigma = \frac{1}{3.31 \times R \times d}, \tag{1}$$

where $3.31 \times R$ is the sheet resistance and d is the pellet thickness, which was measured by a micrometer. A temperature dependence of the conductivity for the HCl-PANI-Fe composite pellet was measured in the temperature range of 55–290 K using the Cryogen-Magnet system with the four-point probe (Cryogenic, CFM-5T-H3-CFVTI-1.6 K-24.5). Thermogravimetric analysis (TGA) (Setaram, Labsy-Evo) was used to study a weight loss of the composite in air at heating temperature up to 400°C. The heating rate was 10°C/min.

3. Results and Discussion

Figure 1 shows XRD patterns of the HCl-PANI pellet and the HCl-PANI-Fe composite pellet. As can be seen from Figure 1, the HCl-PANI pellet and the HCl-PANI-Fe composite pellet have a crystalline structure of emeraldine salt (ES-I) [19]. For the composite, the Fe nanoparticles could not influence the crystalline structure of the HCl-PANI. Furthermore, a weak Fe(110) diffraction peak can be detected at a diffraction angle of about 44.76°. According to the diffraction angle of Fe(110) peak, the lattice constant of the Fe nanoparticles is calculated to be 0.2861 ± 0.0006 nm, which is almost equal to that of

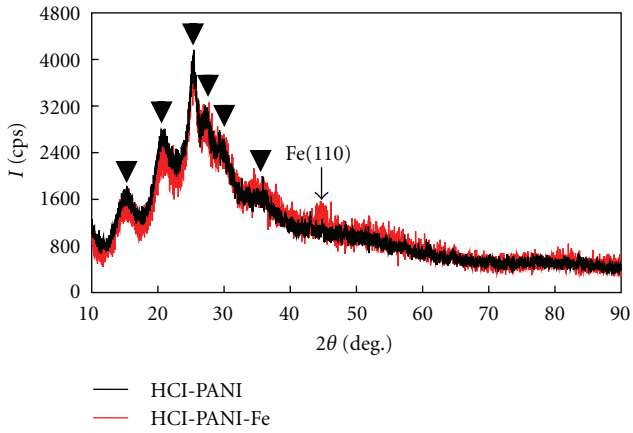

FIGURE 1: XRD patterns of the HCl-PANI pellet and the HCl-PANI-Fe composite pellet. ▼ represents the diffraction peaks of HCl-PNAI.

the Fe bulk (0.28664 nm). No diffraction peaks from the iron oxides are detected.

Figure 2 shows a TEM microphotograph and an electron diffraction (ED) pattern of the HCl-PANI-Fe composite. As can be seen from Figure 2, Fe nanoparticles exist in the composite and some Fe nanoparticles aggregate. The Fe particle size is about 100 nm. These Fe nanoparticles were grown on the HCl-PANI by sputter-depositing. As shown in the ED pattern of Figure 2, Fe(110), Fe(200), and Fe(211) diffraction rings are observed. According to these diffraction rings, the lattice constant of the Fe nanoparticles is calculated to be 0.287 ± 0.003 nm, which is almost equal to that of the Fe bulk (0.28664 nm). The result is consistent with the XRD result. It should be noted that a halo ring shows on the inner side of the Fe(110) diffraction ring. According to the radius of the halo ring, the plane spacing of the atomic short-range order region is estimated to be 0.251 ± 0.002 nm, which is approximate to the plane spacing of Fe_3O_4(311) (0.25312 nm). Therefore, it is considered that the halo ring is attributed to amorphous Fe_3O_4 formed on the Fe nanoparticle surface [20]. Figure 3 shows a high-resolution TEM (HRTEM) image of the HCl-PANI-Fe composite. Using the HRTEM image, the (110) plane spacing of Fe nanoparticle is calculated to be 0.202 ± 0.003 nm. The (110) plane spacing of the Fe nanoparticle is almost equal to that of the Fe bulk (0.20268 nm). This result is consistent with both the XRD and ED results. The HRTEM image definitely shows the Fe nanoparticle formed in the composite.

Figure 4 shows FT-IR spectra of the HCl-PANI and the HCl-PANI-Fe composite. The FT-IR spectroscopy is a powerful tool for analyzing the molecular structure and the oxidation state of PANI [21, 22]. As can be seen from Figure 4, for both the samples, the absorption peak positions of FT-IR spectra are the same. The peak at 1587 cm^{-1} is related to the quinone structure and that at 1471 cm^{-1} is characterized by benzene ring stretching. Therefore, it demonstrates that the aromatic structure of PANI is retained in the HCl-PANI-Fe composite. An intensity ratio of the peak at 1587 cm^{-1} to that at 1471 cm^{-1} is a quantitative measurement of the oxidation

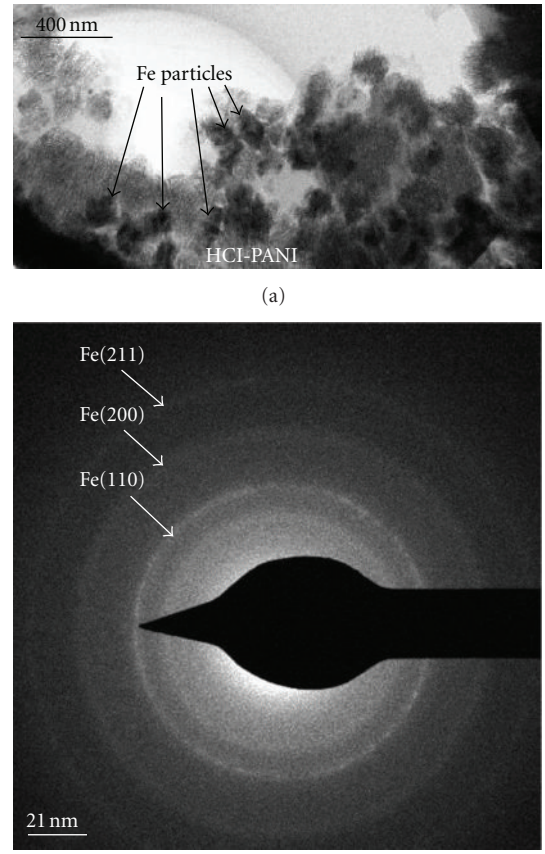

FIGURE 2: TEM microphotograph and ED pattern of the HCl-PANI-Fe composite.

state of PANI [21]. The intensity ratios of the HCl-PANI and HCl-PANI-Fe composite are almost the same, meaning that it does not appear any indication for severe change in the oxidation state for the HCl-PANI-Fe composite. It has been reported that for the PANI-Fe the Fe^{3+} ions coordinate mainly with the nitrogen atoms on the quinone rings leading to the peak of the quinone units shifting to a higher wave numbers compared with the PANI [12]. In this work, however, the peak position at 1587 cm^{-1} related to the quinone units is not influenced by the Fe nanoparticles. It indicates that an interaction between the Fe nanoparticle and the PANI is predominated by a physical mechanism because the Fe nanoparticles are sputter-deposited on the HCl-PANI. Namely, the Fe nanoparticles are physically adsorbed on the HCl-PANI or adhere physically to the HCl-PANI. The peak at 1295 cm^{-1} is also attributed to C–N stretching in the quinoid benzoid rings. The peaks at 1243 and 1115 cm^{-1} result from vibrations in the polar structure of the conducting protonated form [23]. The very weak peak at near 470 cm^{-1} for the HCl-PANI-Fe composite is attributed to the Fe–O interaction [24–26]. However, the characteristic peak at 530–595 cm^{-1} due to the Fe–O stretching band of iron oxide [24–27] cannot be detected. Therefore, it is considered that the Fe nanoparticles are mainly formed in the composite. It is

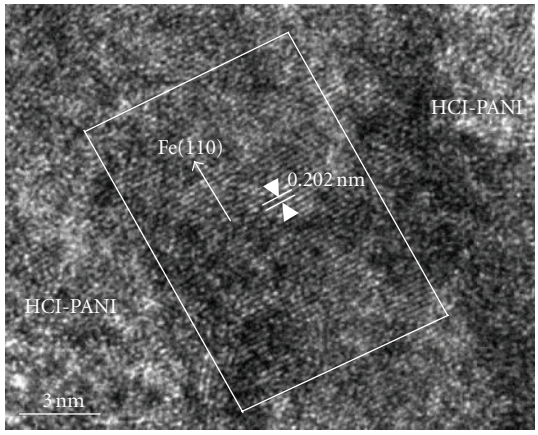

Figure 3: HRTEM image of the HCl-PANI-Fe composite. The (110) plane spacing of Fe nanoparticle is calculated by using the lattice pattern in the rectangular area represented in the figure.

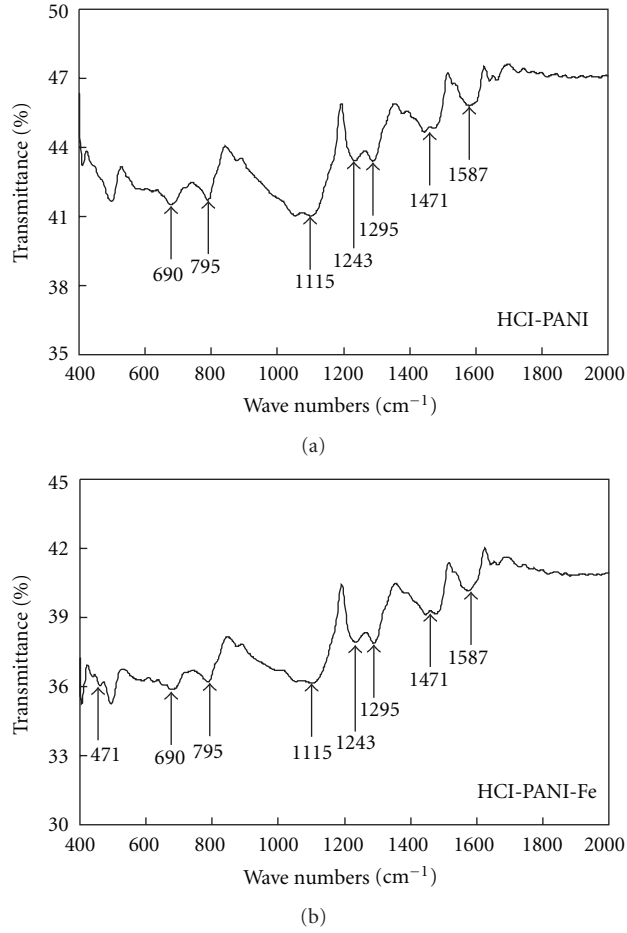

Figure 4: FT-IR spectra of the HCl-PANI and the HCl-PANI-Fe composite.

consistent with the results of XRD, ED, and HRTEM. The very weak peak at near 470 cm^{-1} for the composite might be due to the Fe–O interaction on the Fe nanoparticle surface.

Figure 5 shows a magnetization curve and a temperature dependence of the magnetization for the HCl-PANI-Fe composite pellet. As can be seen from Figure 5, the HCl-PANI-Fe composite pellet exhibits hysteresis, meaning that the composite has room temperature ferromagnetism. As a comparison, a magnetization curve of the HCl-PANI was also measured by VSM. The HCl-PANI does not show the magnetic hysteresis loop [16]. The temperature dependence of the magnetization further proves that the HCl-PANI-Fe composite has the ferromagnetism even over room temperature. A study on organic magnets such as PANI is significant for fundamental and practical viewpoints [28, 29]. It was found that the HCl-PANI exhibited a paramagnetic behavior at 10 K and its paramagnetic behavior gradually changed into diamagnetic with increasing the temperature up to 330 K [30]. It was reported that a new type of polymer produced from polyaniline and tetracyanoquinodimethane was ferrimagnetic or ferromagnetic with a Curie temperature of over 350 K and the magnetically ordered state developed with aging time [31]. The research and development of the organic magnets with a high Curie temperature, which has a magnetic order with strong magnetic interactions, is a challenging work [32]. In the present work, the HCl-PANI-Fe composite, which only contains about 1.66 wt% Fe, has better room temperature ferromagnetism. The saturation field and the coercivity are estimated to be about 4000 Oe and 300 Oe, respectively. The residual magnetization ratio, that is, the ratio of the residual magnetization to the saturation magnetization, is 0.18.

Conductivities of the HCl-PANI pellet and the HCl-PANI-Fe composite pellet are 0.42 S/cm and 0.25 S/cm, respectively. Figure 6 shows a variation of conductivity with temperature for the HCl-PANI-Fe composite pellet, plotted as $\ln\sigma$ versus $T^{-1/4}$. In the variable range hopping (VRH) model [33–35], a temperature T dependence of conductivity σ follows the relation

$$\sigma = \sigma_0 \exp\left[-\left(\frac{T_0}{T}\right)^{1/r}\right], \tag{2}$$

where T_0 is the Mott characteristic temperature and σ_0 is the conductivity at $T = \infty$. T_0 and σ_0 are determined by the localization length, the density of state, and the hopping distance in the material. The r is determined by a dimension of the researching system. For the one-dimensional (1D), two-dimensional (2D), and three-dimensional (3D) systems, r is equal to 2, 3, and 4, respectively. In the 3D-VRH model, (2) can be express as

$$\sigma = \sigma_0 \exp\left[-\left(\frac{T_0}{T}\right)^{1/4}\right]. \tag{3}$$

As can be seen from Figure 6, the plots exhibit a good linear dependence having a correlation coefficient better than 0.9991. It indicates that the 3D-VRH model is suitable for explaining the carrier transport mechanism of the HCl-PANI-Fe composite. It has been reported that for the HCl-PANI the carrier transport mechanism is 3D-VRH [16, 36].

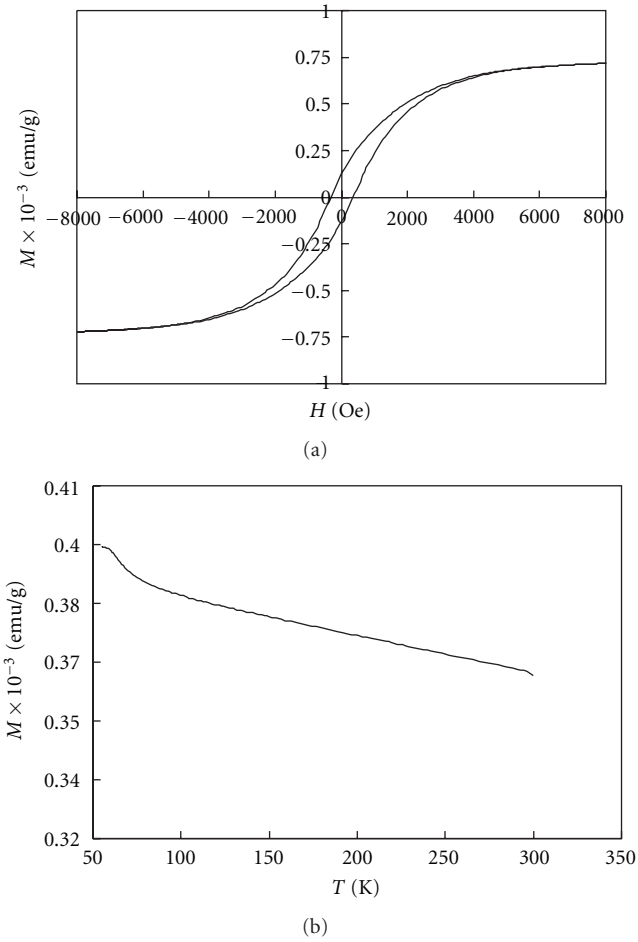

Figure 5: Magnetization curve and temperature dependence of the magnetization for the HCl-PANI-Fe composite pellet.

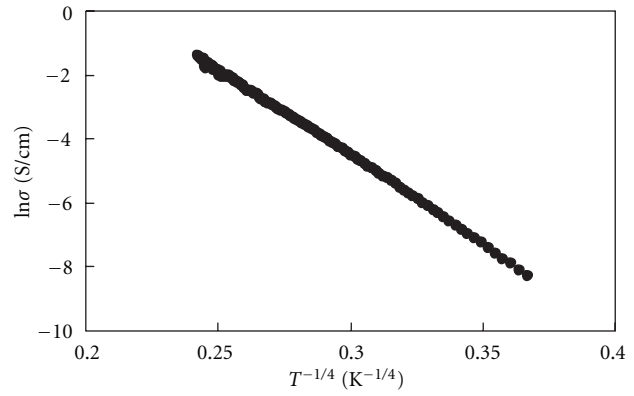

Figure 6: Variation of conductivity with temperature for the HCl-PANI-Fe composite pellet, plotted as lnσ versus $T^{-1/4}$.

Therefore, the Fe nanoparticles do not change the carrier transport mechanism of the HCl-PANI in the HCl-PANI-Fe composite. Values of the T_0 and σ_0 obtained from the fitted straight line of Figure 6 are equal to 8417719 K and 112420 S/cm. Cl^- ions have small size in the HCl-PANI. Then the interchain separation may be small, resulting in an existence of strong coherence/coupling between chains [34]. Therefore, charge carriers could hop from one chain to the other in terms of the 3D-VRH. The Fe nanoparticles are nanosized and the nanoparticle amount is less. Thus, the Fe nanoparticles do not weaken strong coherence/couple between the PANI chains. As a result, for the HCl-PANI-Fe composite, the carrier transport mechanism is also 3D-VRH.

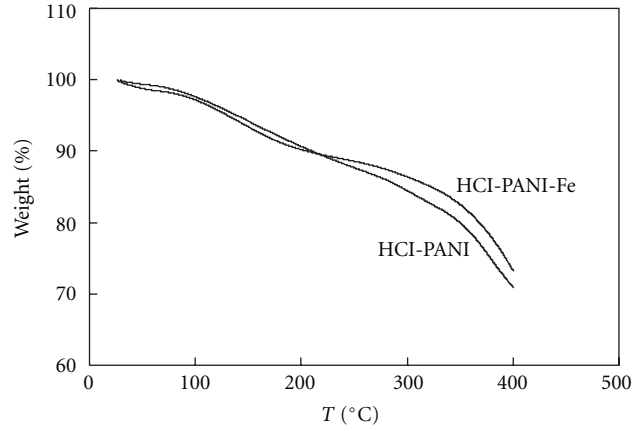

Figure 7: Thermogravimetric curves for the HCl-PANI and the HCl-PANI-Fe composite.

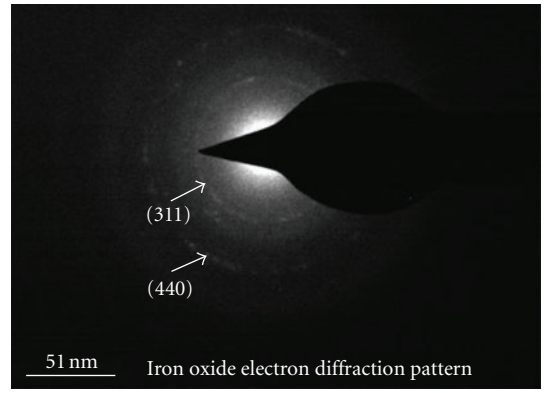

Figure 8: ED pattern of the heat-treated HCl-PANI-Fe composite.

The TGA measurements for the HCl-PANI and the HCl-PANI-Fe composite were carried out in air to study their thermal stability in atmosphere. Figure 7 shows thermogravimetric curves for the HCl-PANI and the HCl-PANI-Fe composite. As can be seen from Figure 7, a three-step weight loss process can be observed for both the samples. The first step at temperatures up to 110°C may be due to the loss of water, the second step in the temperature range of 110–300°C can be attributed to the loss of impurities such as HCl dopant and the third step at the temperatures over 300°C may be due to the degradation of the polymer [37]. Furthermore, it should be noted that for the same heating temperature the weight loss of the HCl-PANI-Fe composite is smaller than that of the HCl-PANI after heating over 230°C. This result is similar to that of the HCl-PANI-Fe composites mixed mechanically [38] but differs from that of the HCl-PANI-Ni composite [16]. The Fe nanoparticles in the composite

might be oxidized during the TGA measurement. In order to confirm the oxidation of the Fe nanoparticles in the HCl-PANI-Fe composite, the composite was heat treated in air at 295°C for 30 minutes. Figure 8 shows an ED pattern of the heat-treated HCl-PANI-Fe composite. As shown in Figure 8, the diffraction rings from the iron oxide are only observed, meaning that the Fe nanoparticles in the composite were oxidized by heat treating. It is consistent with the result reported previously for the HCl-PANI-Fe composites mixed mechanically [38]. Therefore, it is considered that the Fe nanoparticles in the composite are oxidized during TGA measuring. It was reported that heating led to an increase in the weight of the Fe nanoparticles due to the Fe oxidation when the heating temperature exceeded 100°C [20]. Furthermore, it has also been proposed that the PANI-Fe_3O_4 and PANI-Fe_2O_3 composites have a better thermal stability compared with the PANI [6, 9, 39]. However, in the present work, the reason that the weight loss of the HCl-PANI-Fe composite is smaller than that of the HCl-PANI over 230°C is not clear. Detailed work should be further done.

4. Summary

The HCl-PANI-Fe composite was successfully prepared by using the well-established polymerization procedure followed by the sputter-deposition of Fe. The Fe nanoparticle size is about 100 nm. HCl-PANI structure is not influenced by the Fe nanoparticles. The composite pellet has room temperature ferromagnetism and a conductivity of 0.25 S/cm. The carrier transport mechanism in the composite is three-dimensional variable range hopping. The weight loss of the HCl-PANI-Fe composite is smaller than that of the HCl-PANI for the same heating temperature when the temperature exceeds 230°C. Furthermore, this work also confirms the feasibility of the chemically and physically combinative method to prepare the PANI composites containing metal nanoparticles.

Acknowledgments

The authors would like to thank Dr. Xin Gao at the Analysis Center of School of Materials Science and Engineering for supporting TEM and HRTEM observations. The authors would also like to thank Dr. Jinxia Deng at Department of Chemistry for the TGA measurements.

References

[1] M. X. Wan and J. C. Li, "Electrical and ferromagnetic behavior of polyaniline composites," *Synthetic Metals*, vol. 101, no. 1, pp. 844–845, 1999.

[2] J. Deng, X. Ding, W. Zhang et al., "Magnetic and conducting Fe_3O_4-cross-linked polyaniline nanoparticles with core-shell structure," *Polymer*, vol. 43, no. 8, pp. 2179–2184, 2002.

[3] Z. Zhang and M. Wan, "Nanostructures of polyaniline composites containing nano-magnet," *Synthetic Metals*, vol. 132, no. 2, pp. 205–212, 2003.

[4] J. C. Aphesteguy and S. E. Jacobo, "Composite of polyaniline containing iron oxides," *Physica B*, vol. 354, no. 1-4, pp. 224–227, 2004.

[5] Q. Xiao, X. Tan, L. Ji, and J. Xue, "Preparation and characterization of polyaniline/nano-Fe_3O_4 composites via a novel Pickering emulsion route," *Synthetic Metals*, vol. 157, no. 18–20, pp. 784–791, 2007.

[6] Y. J. Zhang, Y. W. Lin, C. C. Chang, and T. M. Wu, "Magnetic properties of hydrophilic iron oxide/polyaniline nanocomposites synthesized by in situ chemical oxidative polymerization," *Synthetic Metals*, vol. 160, no. 9-10, pp. 1086–1091, 2010.

[7] A. C. V. de Araújo, R. J. de Oliveira, S. Alves Júnior et al., "Synthesis, characterization and magnetic properties of polyaniline-magnetite nanocomposites," *Synthetic Metals*, vol. 160, no. 7-8, pp. 685–690, 2010.

[8] M. Petrychuk, V. Kovalenko, A. Pud, N. Ogurtsov, and A. Gubin, "Ternary magnetic nanocomposites based on core-shell Fe_3O_4/polyaniline nanoparticles distributed in PVDF matrix," *Physica Status Solidi A*, vol. 207, no. 2, pp. 442–447, 2010.

[9] K. Singh, A. Ohlan, R. K. Kotnala, A. K. Bakhshi, and S. K. Dhawan, "Dielectric and magnetic properties of conducting ferromagnetic composite of polyaniline with γ-Fe_2O_3 nanoparticles," *Materials Chemistry and Physics*, vol. 112, no. 2, pp. 651–658, 2008.

[10] Z. Wang, H. Bi, J. Liu, T. Sun, and X. Wu, "Magnetic and microwave absorbing properties of polyaniline/γ-Fe_2O_3 nanocomposite," *Journal of Magnetism and Magnetic Materials*, vol. 320, no. 16, pp. 2132–2139, 2008.

[11] C. M. S. Izumi, V. R. L. Constantino, A. M. C. Ferreira, and M. L. A. Temperini, "Spectroscopic characterization of polyaniline doped with transition metal salts," *Synthetic Metals*, vol. 156, no. 9-10, pp. 654–663, 2006.

[12] S. Li, C. Zhu, L. Tang, and J. Kan, "Unique properties of polyaniline in the presence of applied magnetic field and ferric chloride," *Materials Chemistry and Physics*, vol. 124, no. 1, pp. 168–172, 2010.

[13] W. Xue, H. Qiu, K. Fang, J. Li, J. Zhao, and M. Li, "Electrical and magnetic properties of the composite pellets containing DBSA-doped polyaniline and Fe nanoparticles," *Synthetic Metals*, vol. 156, no. 11–13, pp. 833–837, 2006.

[14] S. Kreuzer, K. Prügl, G. Bayreuther, and D. Weiss, "Epitaxial growth and patterning of sputtered Fe films on GaAs(001)," *Thin Solid Films*, vol. 318, no. 1-2, pp. 219–222, 1998.

[15] C. Quintana, J. L. Menéndez, Y. Huttel, M. Lancin, E. Navarro, and A. Cebollada, "Structural characterization of Fe(1 1 0) islands grown on α-Al2O3(0 0 0 1)," *Thin Solid Films*, vol. 434, no. 1-2, pp. 228–238, 2003.

[16] R. Liu, H. Qiu, H. Li, H. Zong, and C. Fang, "Fabrication and characteristics of composite containing HCl-doped polyaniline and Ni nanoparticles," *Synthetic Metals*, vol. 160, no. 23-24, pp. 2404–2408, 2010.

[17] P. N. Adams, P. J. Laughlin, A. P. Monkman, and A. M. Kenwright, "Low temperature synthesis of high molecular weight polyaniline," *Polymer*, vol. 37, no. 15, pp. 3411–3417, 1996.

[18] "Standard test method for sheet resistance of thin metallic films with a collinear four-probe array," ASTM International, West Conshohocken, F390-98, 2003.

[19] M. E. Jozefowicz, R. Laversanne, H. H. S. Javadi et al., "Multiple lattice phases and polaron-lattice spinless-defect competition in polyaniline," *Physical Review B*, vol. 39, no. 17, pp. 12958–12961, 1989.

[20] C. J. Choi, O. Tolochko, and B. K. Kim, "Preparation of iron nanoparticles by chemical vapor condensation," *Materials Letters*, vol. 56, no. 3, pp. 289–294, 2002.

[21] G. E. Asturias, A. G. MacDiarmid, R. P. McCall, and A. J. Epstein, "The oxidation state of "emeraldine" base," *Synthetic Metals*, vol. 29, no. 1, pp. 157–162, 1989.

[22] J. Tang, X. Jing, B. Wang, and F. Wang, "Infrared spectra of soluble polyaniline," *Synthetic Metals*, vol. 24, no. 3, pp. 231–238, 1988.

[23] J. Prokeš, M. Trchová, D. Hlavatá, and J. Stejskal, "Conductivity ageing in temperature-cycled polyaniline," *Polymer Degradation and Stability*, vol. 78, no. 2, pp. 393–401, 2002.

[24] A. Šarić, S. Musić, K. Nomura, and S. Popović, "FT-IR and ^{57}Fe Mossbauer spectroscopic investigation of oxide phases precipitated from $Fe(NO_3)_3$ solutions," *Journal of Molecular Structure*, vol. 480-481, pp. 633–636, 1999.

[25] M. Ristić, E. De Grave, S. Musić, S. Popović, and Z. Orehovec, "Transformation of low crystalline ferrihydrite to α-Fe_2O_3 in the solid state," *Journal of Molecular Structure*, vol. 834–836, pp. 454–460, 2007.

[26] M. Žic, M. Ristić, and S. Musić, "Precipitation of α-Fe_2O_3 from dense β-FeOOH suspensions with added ammonium amidosulfonate," *Journal of Molecular Structure*, vol. 924–926, pp. 235–242, 2009.

[27] K. R. Reddy, K. P. Lee, and A. I. Gopalan, "Self-assembly approach for the synthesis of electro-magnetic functionalized Fe_3O_4/polyaniline nanocomposites: effect of dopant on the properties," *Colloids and Surfaces A*, vol. 320, no. 1–3, pp. 49–56, 2008.

[28] A. J. Epstein and J. S. Miller, "Molecule- and polymer-based magnets, a new frontier," *Synthetic Metals*, vol. 80, no. 2, pp. 231–237, 1996.

[29] J. A. Crayston, J. N. Devine, and J. C. Walton, "Conceptual and synthetic strategies for the preparation of organic magnets," *Tetrahedron*, vol. 56, no. 40, pp. 7829–7857, 2000.

[30] P. Dallas, D. Stamopoulos, N. Boukos, V. Tzitzios, D. Niarchos, and D. Petridis, "Characterization, magnetic and transport properties of polyaniline synthesized through interfacial polymerization," *Polymer*, vol. 48, no. 11, pp. 3162–3169, 2007.

[31] N. A. Zaidi, S. R. Giblin, I. Terry, and A. P. Monkman, "Room temperature magnetic order in an organic magnet derived from polyaniline," *Polymer*, vol. 45, no. 16, pp. 5683–5689, 2004.

[32] D. Luneau, "Molecular magnets," *Current Opinion in Solid State and Materials Science*, vol. 5, no. 2-3, pp. 123–129, 2001.

[33] M. Gosh, A. Barman, A. K. Meikap, S. K. De, and S. Chatterjee, "Hopping transport in HC1 doped conducting polyaniline," *Physics Letters A*, vol. 260, no. 1-2, pp. 138–148, 1999.

[34] Z. H. Wang, H. H. S. Javadi, A. Ray, A. G. MacDiarmid, and A. J. Epstein, "Electron localization in polyaniline derivatives," *Physical Review B*, vol. 42, no. 8, pp. 5411–5414, 1990.

[35] W. Li and M. Wan, "Porous polyaniline films with high conductivity," *Synthetic Metals*, vol. 92, no. 2, pp. 121–126, 1998.

[36] J. Li, K. Fang, H. Qiu, S. Li, and W. Mao, "Micromorphology and electrical property of the HCl-doped and DBSA-doped polyanilines," *Synthetic Metals*, vol. 142, no. 1–3, pp. 107–111, 2004.

[37] G. M. Do Nascimento, C. H. B. Silva, and M. L. A. Temperini, "Spectroscopic characterization of the structural changes of polyaniline nanofibers after heating," *Polymer Degradation and Stability*, vol. 93, no. 1, pp. 291–297, 2008.

[38] G. Ren, H. Qiu, Q. Wu, H. Li, H. Fan, and C. Fang, "Thermal stability of composites containing HCl-doped polyaniline and Fe nanoparticles," *Materials Chemistry and Physics*, vol. 120, no. 1, pp. 127–133, 2010.

[39] S. S. Umare, B. H. Shambharkar, and R. S. Ningthoujam, "Synthesis and characterization of polyaniline-Fe_3O_4 nanocomposite: electrical conductivity, magnetic, electrochemical studies," *Synthetic Metals*, vol. 160, no. 17-18, pp. 1815–1821, 2010.